Biochimica et Biophysica Acta 1848 (2015) 151–158

Contents lists available at ScienceDirect

Biochimica et Biophysica Acta

journal homepage: www.elsevier.com/locate/bbamem

Modulation of the mitochondrial voltage dependent anion channel (VDAC) by curcumin

Debanjan Tewari [a], Tofayel Ahmed [a,1,2], Venkat R. Chirasani [a,1], Pradeep K. Singh [b], Samir K. Maji [b], Sanjib Senapati [a], Amal Kanti Bera [a,*]

[a] Department of Biotechnology, Bhupat and Jyoti Mehta School of Biosciences Building, Indian Institute of Technology Madras, Chennai 600036, India
[b] Department of Biosciences and Bioengineering, Indian Institute of Technology Bombay, Powai, Mumbai 400076, India

ARTICLE INFO

Article history:
Received 31 July 2014
Received in revised form 6 October 2014
Accepted 13 October 2014
Available online 23 October 2014

Keywords:
Ion channel
VDAC
Gating
Curcumin
Apoptosis
Mitochondria

ABSTRACT

Voltage dependent anion channel (VDAC) of mitochondria plays a crucial role in apoptosis. Human VDAC-1, reconstituted in planar lipid bilayer showed reduced conductance when treated with curcumin. Curcumin interacts with residues in the α helical N-terminus of VDAC and in the channel wall, as revealed by molecular docking, followed by mutational analysis. N-terminus mimicking peptide showed conformational changes in circular dichroism, upon curcumin treatment. We propose that the interaction of curcumin with amino acids in N-terminus and in channel wall fixes the α helix in closed conformation. This restricts its movement which is required for the opening of the channel.

1. Introduction

Voltage dependent anion channel (VDAC) is the most abundant protein in the outer mitochondrial membrane [1–3]. It serves as a primary conduit between cell cytoplasm and mitochondria, facilitating the exchange of ions and important biomolecules like ATP, ADP, pyruvate and succinate [4–6]. Recent crystal structure reveals that the major structural components of VDAC include 19 β strands and an N-terminal α helix. 19 β strands constitute the β barrel and the N-terminal α helix resides within the pore [7]. VDAC assumes an open conformation at lower membrane potentials and closed state at potentials more than ±20 mV. Unlike other channels, VDAC rarely exhibits fully closed, nonconductive state and thus the 'closed state' often refers to sub-conductance state which is still permeable to small ions. Open state is anion selective while closed state prefers cations [4,8]. Although there are controversies, large number of evidences support that the N-terminus participates in the gating of VDAC [8–12]. Flexibility and strategic location of the α helix within the pore prompted the hypothesis that channel opening is accompanied by the displacement of the helix from its central position to the inner wall [13]. Alternatively, outward movement of the α helix has also been proposed [14]. Teijido et al. proposed the gating of VDAC without participation of N-terminal α helix [15].

VDAC plays a major role in mitochondria mediated apoptosis [3,6,16,17]. Several anti-apoptotic and pro-apoptotic proteins as well as chemicals are known to target VDAC [18–20]. Intra-mitochondrial calcium overload mediated by VDAC, triggers the formation of permeability transition pore (PTP). Increased mitochondrial permeability is followed by the release of cytochrome c to the cytosol which in turn activates the death process [21,22]. Glycolytic enzyme hexokinase (HK), particularly in cancer cells interacts with the N-terminus of VDAC and offers protection against apoptosis [23]. Disruption of VDAC-HK interaction enhances the sensitivity of cancer cells to chemotherapeutic agents [6]. Anti-apoptotic protein Bcl-xL directly interacts with VDAC [24]. Anti VDAC-1 antibody prevented As_2O_3 induced cytochrome c release in isolated mitochondria and Bax induced apoptosis in intact cells [25]. Similarly, down regulation of VDAC-1 by siRNA prevented cisplatin induced Bax activation and cell death [26].

Curcumin, a pigmented polyphenolic compound is known to have anticancer activity [27]. It up-regulates pro-apoptotic proteins like Bax and down regulates anti-apoptotic proteins, Bcl-2 and Bcl-xl [28]. The down-regulation of anti-apoptotic proteins promotes the death process by sensitizing cells to increase mitochondrial calcium, ROS generation, cytochrome c release and activation of caspases [27–29]. Many ion channels and transporters e.g. voltage gated potassium channels

Abbreviations: VDAC, voltage dependent anion channel; HK, hexokinase; CD, circular dichroism

* Corresponding author. Tel.: +91 44 2257 4121; fax: +91 44 2257 4102.
E-mail address: amal@iitm.ac.in (A.K. Bera).

[1] These authors contributed equally.

[2] Present Addresses: Nanyang Technological University, Division of Structural Biology and Biochemistry, Singapore.

http://dx.doi.org/10.1016/j.bbamem.2014.10.014
0005-2736/

(Kv1.3, Kv11.1), CFTR chloride channel, voltage gated calcium channels, ABC transporters and glucose transporters are modulated by curcumin [30] Curcumin-induced release of 'apoptosis inducing factor' (AIF) involves VDAC [31]. Although curcumin is known to modulate various proteins associated with cell survival and death, its direct effect on VDAC has not been studied. We show that curcumin induces closure of reconstituted hVDAC-1 in planar lipid bilayer. The key residues of VDAC that interact with curcumin are identified and the possible mechanism of VDAC-closure is discussed.

2. Materials and methods

2.1. Materials

Escherichia coli M15 (pREP4) bacterial strain and Ni-NTA matrix were purchased from Qiagen. Tris-Hcl, Guanidine HCl, Trition X-100 and DTT (Dithiothreitol) were obtained from HiMedia, India. LDAO (N,N-Dimethyldodecylamin-N-oxide) was purchased from Sigma Chemicals, USA. Hydroxylapatite and celite were purchased from Bio-Rad, USA. Curcumin was obtained from Loba Chime, India.

2.2. Expression and purification of VDAC

Recombinant His-tag hVDAC-1 was expressed in *E. coli* M15 (pREP4). VDAC expression was induced with 1 mM IPTG. Harvested cells were ruptured by sonication in the buffer containing 150 mM NaCl, 30 mM Tris– HCl (pH 8). The lysate was centrifuged at 4800 ×*g* for 30 min at 4 °C. The pellet was washed in the buffer containing 2% Triton X-100. The purified inclusion bodies were dispersed in buffer containing 6 M Guanidine HCl, 10 mM DTT, 0.1 mM EDTA and 100 mM Tris–HCl (pH 8). The extracted protein was re-folded in buffer containing 0.1 mM EDTA, 1 mM DTT, 100 mM Tris–HCl (pH 8) and 2% LDAO. The protein solution was centrifuged at 150,000 ×*g* for 45 min. The supernatant was dialyzed twice against phosphate buffer (pH 6) containing 0.1% LDAO for 24 h. His-tag VDAC was purified using Ni-NTA column as described before [32]. Bovine brain VDAC was purified using hydroxylapatite-celite column as described before [33].

2.3. SDS-PAGE and Western blotting

Homogeneity of the purified VDAC was checked on SDS-PAGE. Purified protein sample was resolved on 12% gel as per standard Lammeli's method, followed by silver staining [34]. Molecular weight of the purified hVDAC-1 was compared using standard molecular weight marker (BioRad). For western blot, 20 μg of purified hVDAC-1 was resolved on SDS-PAGE. After electrophoresis, proteins were transferred to polyvinylidene fluoride (PVDF) membrane (Bio-Rad, USA), and then blocked with 5% bovine serum albumin (BSA) and 0.1% Tween-20 in Tris-buffered saline (TBS) for 1 h at room temperature (22 °C–24 °C). The blot was incubated overnight at 4 °C with monoclonal antibody against hVDAC-1 (Cell Signaling Technologies, USA) at 1:750 dilution. After several washes with TBS-Tween-20 solution, the blot was incubated for 1 h with HRP-conjugated secondary antibody (GeNei, Lot No: 031062) at 1:5000 dilution. The blot was treated with super signal west pico-chemiluminescent substrate (Thermo Scientific, USA) and visualized on X-ray film (Amersham, USA).

2.4. Site directed mutagenesis

The mutants of hVDAC-1: K15A, R18A, D19A and Y198F were created using Quick Change mutagenesis kit (Stratagene, La Jolla, CA, USA) according to the manufacturers' protocol. The primers used for generating the mutants are shown in Supplementary Table 1. The mutation was confirmed by sequencing.

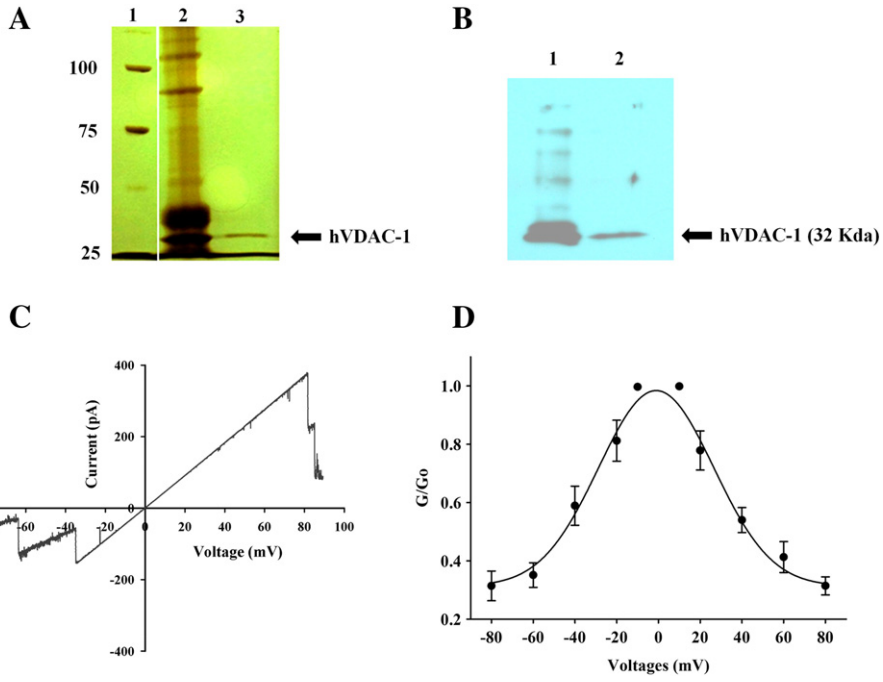

Fig. 1. Characterization of purified hVDAC-1. A. SDS-PAGE profile of purified hVDAC-1. 20 μg of purified protein was resolved on 12% polyacrylamide gel, followed by silver staining. Molecular weight of purified hVADC-1 appeared to be around 32 KDa. Lane 1, standard molecular weight marker; Lane 2, Fraction after refolding; Lane 3, purified hVDAC-1. B. Western blot confirming the purified protein as hVDAC-1. Lane 1, fraction after re-folding; Lane 2, purified hVDAC-1. C. Representative current voltage (I-V) plot of hVDAC-1. I-V plot was generated using a voltage ramp from −90 mV to +90 mV. Closing events are observed at higher voltages. D. Relative conductance (G: conductance at a given voltage; G_0: maximum conductance) versus voltage plot of hVDAC-1. Relative conductance decreased with increasing voltages, a typical signature of VDAC. Values are the mean ± SEM of 10 independent observations. Solid line represents fitted curve, generated using Gaussian function (Sigma plot 11).

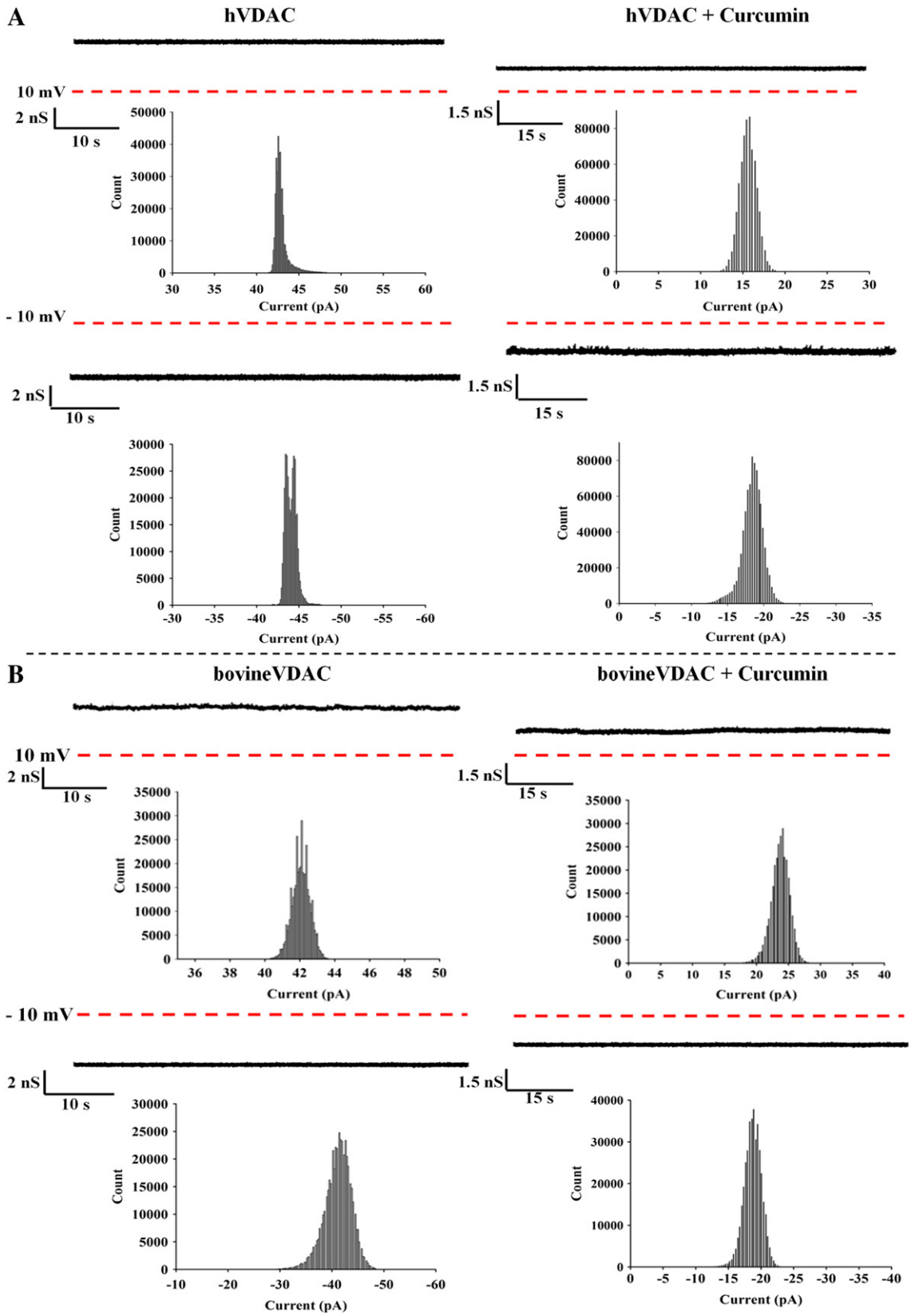

Fig. 2. Effect of Curcumin on VDAC-1. A. Representative current traces recorded at + 10 mV/— 10 mV and respective all point histograms (below the current traces) are presented. Current value decreased when 50 μM of curcumin was added to the *cis* side. Left panel shows control hVDAC-1 without curcumin. B. Current traces recorded from bovine brain VDAC. Dotted lines in red represent base line (0 pA) and the holding potentials are indicated in the left.

2.5. Reconstitution of VDAC in planar lipid bilayer

Purified VDAC was reconstituted in planer lipid bilayer as described before [35]. Briefly, the bilayer was formed with 1,2-diphytanoyl-sn-glycero-3 phosphatidyl choline (DPhPC) (Avanti Polar Lipids, Alabaster, AL), dissolved in n-decane (20 mg/ml). Lipid was painted on the aperture (150 μm diameter) of polystyrene bilayer cuvette (Warner Instrument, USA). Both *cis* and *trans* chambers contained symmetrical solution of 1 M KCl, 5 mM $MgCl_2$ and 10 mM HEPES (pH 7.4). The *cis* chamber was held at virtual ground and the *trans* chamber was connected to the recording amplifier through PC501A head-stage (Warner Instrument, USA). Ag-AgCl electrodes were used. After formation of stable bilayer, purified VDAC was added to the *cis* chamber and the solution was mixed with magnetic stirrer. Channel insertion was monitored by observing membrane currents at different voltages. Once the channel insertion was noticed, the solution of *cis* chamber was replaced with fresh solution to limit further insertion of channels. To check the effect of curcumin, it was added to the *cis* chamber (50 μM final concentration). Channel activity was recorded at different voltages before and after the addition of curcumin. Currents were low pass filtered at 1 kHz and digitized at 5 kHz. The pClamp software (version 9, Molecular Devices) was used for data acquisition and analysis.

2.6. Protein-ligand docking

Docking studies were performed to locate the probable binding site of curcumin on VDAC. Docking analysis was carried out using Autodock 4.2 [36]. The structure of VDAC was obtained from Protein Data Bank (PDB ID: 2JK4) [37] and the chemical structure of curcumin was retrieved from PubChem data base (ID: 969516). A total of 100 binding conformations were generated by docking curcumin in the flexible form to VDAC crystal structure. Polar hydrogens were added to the protein structure and Kollman united atom partial charges were assigned to both protein and ligand. The grid box was taken sufficiently large at 90 Å × 90 Å × 90 Å, keeping the protein at the center, to ensure unbiased docking. Genetic Algorithm was used and the docked complexes were scored based on binding free energy of the ligand to protein.

2.7. UV–visible spectroscopy

To evaluate the interaction of N-terminal fragment of VDAC with curcumin, we measured the absorbance of curcumin in the presence and absence of the peptide. The peptide, corresponding to the N-terminal first 21 amino acids of VDAC was synthesized by M/S Genpro Biotech, New Delhi, India. For UV–visible spectroscopy, the molar ratio of peptide and curcumin was kept 1:1 (50 μM of each) and spectra were recorded in the range of 300–700 nm using JASCO spectrophotometer. The base line was corrected using respective buffer.

2.8. Circular dichroism (CD) spectroscopy

The peptide containing N-terminal first 21 amino acids of hVDAC-1 was used for CD spectroscopy. CD spectroscopy of the peptide with and without curcumin was performed in phosphate buffer saline (PBS) as well as in methanol. 50 μM of peptide (dissolved in PBS) was incubated with equimolar curcumin for 30 min in dark at room temperature. For CD spectroscopy, the peptide was dissolved in methanol and treated with varying concentrations of curcumin (0–1 μM, in methanol) in dark for 10 min at room temperature [38]. For secondary structural analysis, 200 μl of incubated sample was placed into a 0.1 cm path-length quartz cell (Hellma, Forest Hills, NY) and the spectra were acquired at 25 °C in far-UV range (198 nm–260 nm) with JASCO J-810 CD polarimeter. Three independent measurements were performed with each sample. To calculate the secondary structural component, the CD data were deconvoluted using CDPro software package. This software contains three algorithms (CONTINLL, SELCON3, and CDSSTR) for determining the relative secondary structural components [39].

3. Results

3.1. Effect of curcumin on hVDAC-1

The purity of isolated protein was checked on SDS-PAGE, followed by silver staining. As shown in Fig. 1A, VDAC-1 appeared as ~32 kDa single band on SDS-PAGE, confirming its homogeneity. Further, to establish the identity of hVDAC-1, western blot was performed with anti VDAC-1 antibody. Western blot showed prominent hVDAC-1 band (Fig. 1B). For functional characterization, VDAC-1 was reconstituted in planar lipid bilayer. Purified protein was added to the *cis* compartment (10 μg/ml, final concentration) and the channel insertion was monitored by measuring membrane currents at different voltages. Current–voltage (I–V) plot of VDAC-1 is shown in Fig. 1C. Channels show distinct closing events at higher voltages. This is a well known property of hVDAC-1 [4,8]. Normalized conductance (G/G_0) versus voltage plot of VDAC is shown in Fig. 1D. In agreement with previous reports, relative conductance is highest at voltages around 0 mV and it decreased almost symmetrically with the increase of positive and negative voltages [4,8].

The effect of curcumin on reconstituted VDAC-1 was studied by adding it to the *cis* chamber (50 μM, final concentration). Representative current traces recorded at +/− 10 mV are shown in Fig. 2. Membrane currents reduced significantly after curcumin treatment, implicating that curcumin induces channel closure. Equal volume of vehicle (DMSO) alone had no effect on VDAC-1. Like the recombinant protein, VDAC isolated from bovine brain mitochondria had also showed similar effect (Fig. 2B). Fig. 3 depicts single channel conductance of VDAC-1 measured at different voltages before and after curcumin treatment. Curcumin treated VDAC-1 showed reduced conductance at all voltages. Single channel conductance (in 1 M KCl) at +10 mV was 4.5 ± 0.2 nS which reduced to 1.8 ± 0.15 nS after curcumin treatment.

3.2. Molecular docking of curcumin on hVDAC-1

We have performed protein-ligand docking to understand the mode of curcumin binding and to locate the VDAC residues that might play crucial roles in curcumin binding. Docking was performed by probing the curcumin molecule all across the VDAC-1 surface and N-terminal

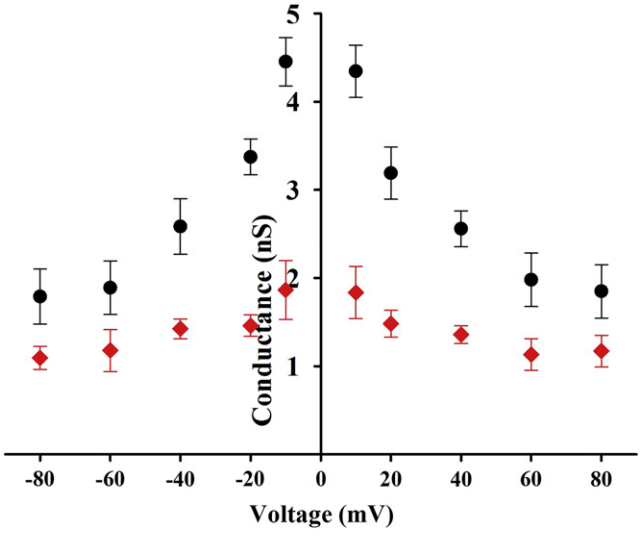

Fig. 3. Effect of curcumin on single channel conductance of hVDAC-1. Curcumin decreased single channel conductance in all test voltages. Control data are shown in black and curcumin treated data are in red. Values are the mean ± SEM of 15 independent experiments.

α helix region (unbiased docking). The binding conformations of curcumin were clustered based on their free energy of binding. Nearly 30% of the curcumin conformations were found to fall in the lowest energy cluster, with an average energy of −7.5 kcal/mol (Supplementary Fig. S1). Detailed structural analysis on the representative conformation from this cluster showed that curcumin preferentially binds to the N-terminal α helix region with a bridging interaction to VDAC wall. In this mode of binding, hydrogen bonding interactions with N-terminal α helix residues K15 and R18 were involved. A stacking interaction between Y198 and one of the phenyl rings of curcumin was also found to play a crucial role in the binding (Fig. 4A). Further analysis revealed the existence of multiple, relatively weaker hydrophobic interactions with VDAC N-terminal and wall residues. This is shown in Fig. 4B. Based on these findings, we selected K15, R18, D19 on N-terminus and Y198 on the channel wall for mutational studies to assess their contribution in curcumin binding.

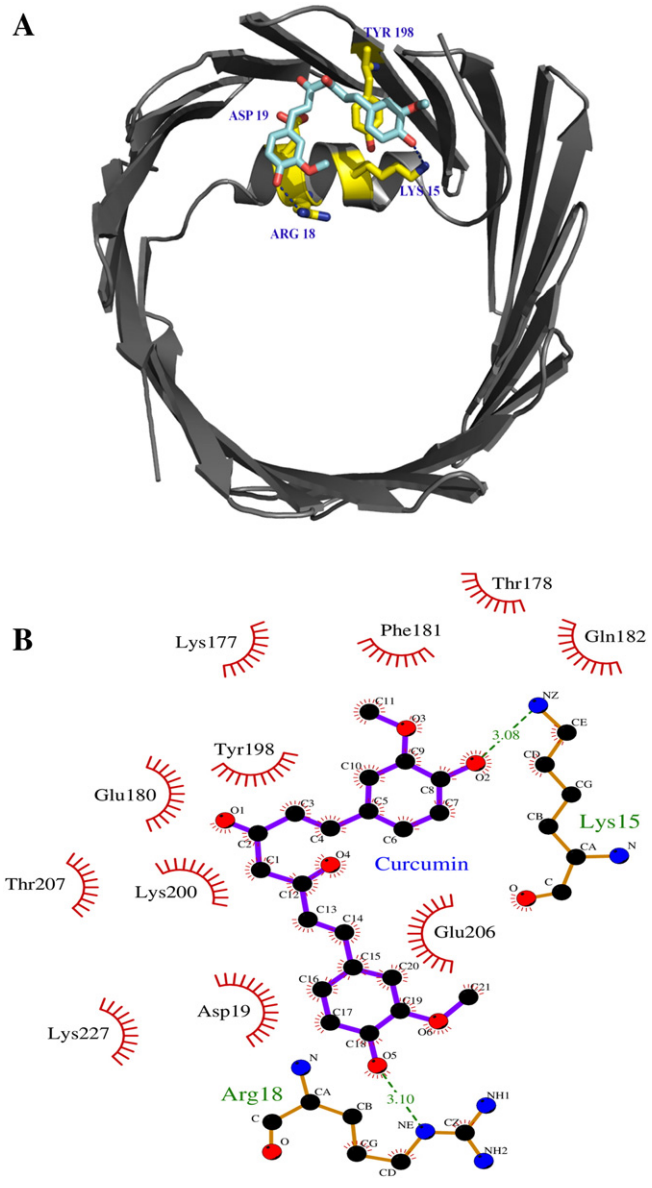

Fig. 4. A. The 3D representation of curcumin binding to hVDAC-1. hVDAC-1 is represented in gray cartoon and curcumin is shown in cyan licorice. Interacting hVDAC-1 residues are depicted in licorice representation in yellow. The electronegative oxygen and nitrogen atoms in curcumin and protein residues are shown in red and blue, respectively. Hydrogen bonds between curcumin and VDAC residues are indicated by dotted lines. B. Interactions of hVDAC-1 residues with curcumin. The hydrogen bonding interactions of curcumin with VDAC residues K15 and R18 are shown by dotted lines. The other protein residues that involve in hydrophobic interactions with curcumin are also indicated.

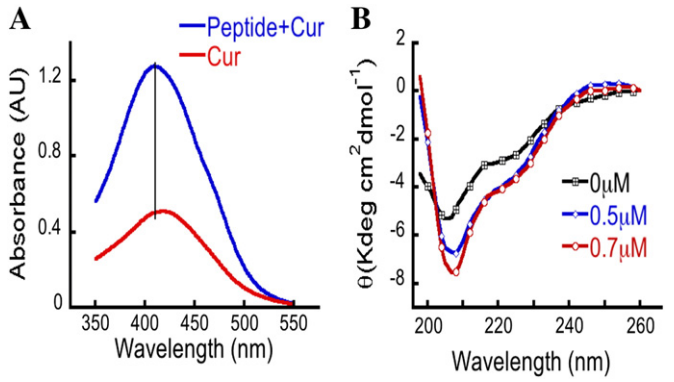

Fig. 5. A. Absorbance spectra of curcumin (50 μM) in the presence and absence of equimolar concentration of peptide. An increase in curcumin absorbance intensity and a prominent blue shift in its absorbance maxima were observed in the presence of peptide. B. CD spectra of peptide (40 μM) with varying concentration of curcumin in methanol. As evident in CD spectra, peptide adopted α helical conformation in methanol and curcumin treatment increased its helical content.

3.3. Curcumin increases the helicity of synthetic peptide

The docking study identified multiple residues in N-terminus of hVDAC-1 that may interact with curcumin. To study the interaction, 50 μM of synthetic peptide, consisting of 21 amino acids of N-terminus was incubated with equimolar concentration of curcumin for 30 min at room temperature and the absorbance was measured. In presence of the peptide, the curcumin spectrum showed three-fold increase in absorbance with blue shift in the absorption maxima (Fig. 5A). The data clearly suggests that curcumin interacts with the peptide. The same method had been used earlier to demonstrate curcumin-protein interaction [40]. Further, we assumed that synthetic peptide corresponding to the N-terminus, might exhibit some conformational changes induced by curcumin. However, the CD spectra of 50 μM peptide in PBS showed mostly unstructured random coil conformation and its treatment with equimolar concentration of curcumin did not show any significant structural changes (Supplementary Fig. S2). It suggests that though the peptide has propensity for helix formation, it might need some helix favoring conditions for adapting the helical conformation. Therefore, we performed the CD experiment in methanol, which favors helix formation in peptides. The data suggest that peptide exhibited helix conformation in methanol, as evident by two minima (at 222 nm and ~208 nm; Fig. 5B). CD spectra presented in Fig. 5B revealed that helical content of peptide increased with increasing concentrations of curcumin. The change in peptide helicity was observed even at very low curcumin concentration (0.5 μM) in methanol. The helicity of the peptide alone was found to be 8.1% which increased to 11.0%, 15.36% and 20.65% by 0.5 μM, 0.7 μM and 1.0 μM curcumin respectively as calculated from CD Pro deconvolution (Table 1). The CD spectroscopy measurements clearly suggest that

Table 1
Alteration of the secondary structure of N terminal peptide in the presence of curcumin.

Curcumin (μM)	α-Helix (%)	β sheet (%)	Turn (%)	Random coil (%)
0	8.1	31.06	14.26	41.56
0.5	11.03	30.83	16.93	37.0
0.7	15.36	28.83	17.9	35.76
1.0	20.65	34.43	15.5	43.4

The experiment was performed in methanol and the peptide concentration was kept constant (40 μM).

Table 2
Effect of curcumin on single channel conductance of wild type and mutant VDAC. Conductance was calculated at +80 mV in 1 M symmetric KCl solution. * $P < 0.05$, ** $P < 0.01$.

hVDAC-1	Single channel conductance (nS) ± SEM	% reduction of conductance after curcumin treatment
Wild type	2.09 ± 0.10	51
Wild type + curcumin	1.10 ± 0.04**	
K15A	1.85 ± 0.09	30
K15A + curcumin	1.30 ± 0.08*	
R18A	2.08 ± 0.07	33
R18A + curcumin	1.39 ± 0.05*	
D19N	1.91 ± 0.14	27
D19N + curcumin	1.38 ± 0.10*	
Y198F	2.04 ± 0.12	39
Y198F + curcumin	1.25 ± 0.06*	

curcumin increases the helical content of this peptide in suitable environment.

3.4. Effect of curcumin on the mutant hVDAC-1

All the mutants of VDAC-1 i.e. K15A, R18A, D19N, Y198F except K227A readily formed channel in planer lipid membrane. K227A did not show any channel activity. Mutation did not cause any major changes in the electrophysiological properties of VDAC, other than slight decrease of single channel conductance for K15A and D19N. At 80 mV (in 1 M KCl), K15A showed single channel conductance of 1.85 nS compared to 2.09 nS for wild type (Table 2). The effect of curcumin on different mutants of hVDAC-1 at −10 mV holding potential is shown in Fig. 6. Like wild type, curcumin induced the closure to all mutants. However, when the effects of curcumin on single channel conductance of mutants were compared, it appears that mutants are less responsive to curcumin (Table 2). For example, at 80 mV (in 1 M KCl) wild type hVDAC-1 showed a conductance of about 2.09 nS which reduced by 51% upon curcumin treatment. On the other hand, reduction of the conductance for mutants ranged between 28 and 39%, implying that mutation attenuated the effect of curcumin, but did not abolish it completely. Similar effect of the curcumin was also observed at lower holding potentials.

4. Discussion and conclusion

The present study describes alteration of the gating of VDAC by curcumin. Curcumin is a well-known pro-apoptotic agent and it has been extensively studied in relation to its anti-cancer effect [27]. It has

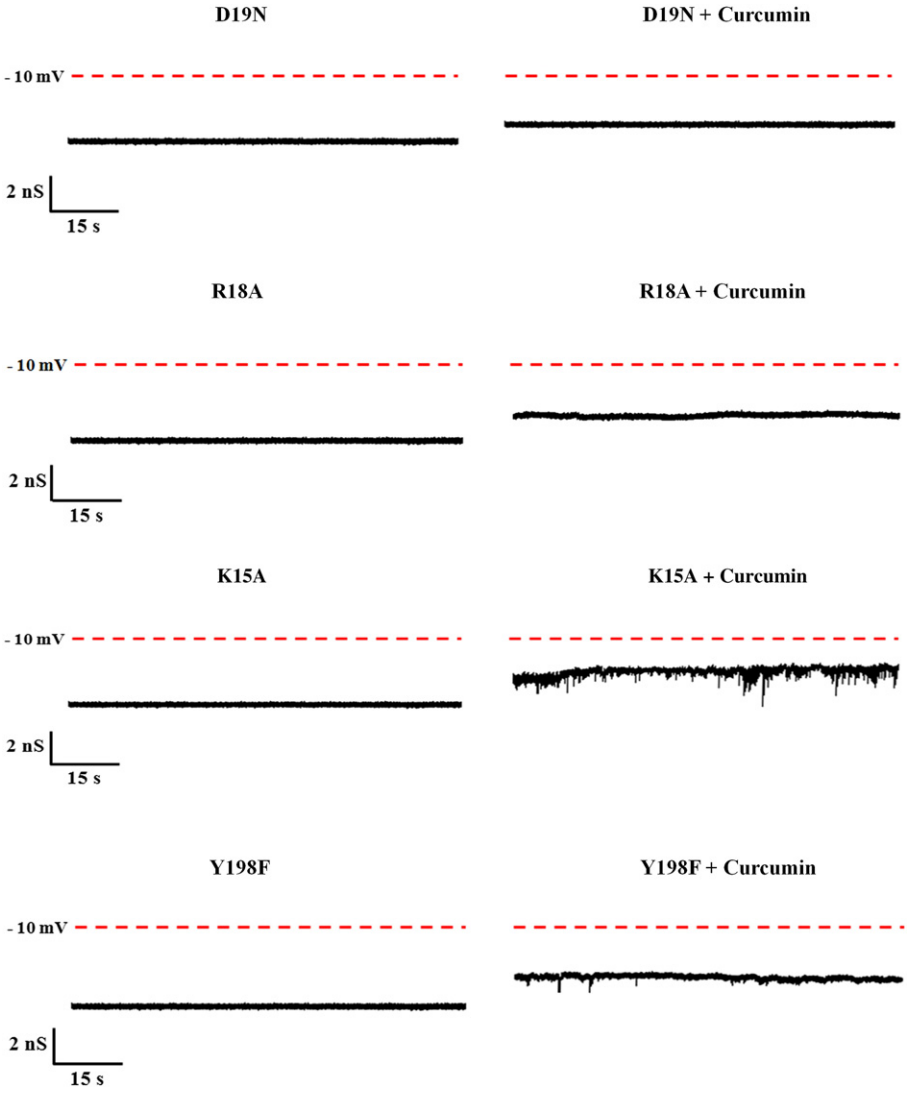

Fig. 6. Effect of curcumin on different VDAC mutants. VDAC was reconstituted in DPhPC membrane and channel activity was recorded in 1 M symmetric KCl solution. Red dotted line represents base line (0 pA); applied voltages are written alongside. Application of curcumin induces closure in all mutants; however the extent of inhibition is significantly lower than wild type (Table 2).

multiple targets like inflammatory cytokines, growth factors, kinases, transcription factors, different ion channels, transporters and wide range of proteins involved in apoptosis pathway [27–30]. Although VDAC plays a central role in mitochondria mediated apoptosis, its modulation by curcumin has never been reported. Here we show that curcumin directly interacts with hVDAC-1 and induces its closure. hVDAC-1 reconstituted in planar lipid bilayer showed reduced conductance when treated with curcumin. Further, molecular docking identified interacting residues, mostly in the N-terminal α helix and in the inner wall of the channel forming β barrel. The synthetic peptide mimicking N-terminus showed interaction with curcumin as evident from curcumin absorbance measurement study. Also, the helicity of this peptide increased with increasing concentration of curcumin, as detected in CD spectroscopy. Curcumin increased the helicity of the peptide, suggesting its specific interaction. Based on the docking data, when the predicted interacting residues of N-terminus i.e. Lys15, Arg18 were mutated to Ala and Asp19 to Asn, all the single mutants of VDAC showed reduced sensitivity to curcumin, suggesting their involvement in binding. As binding of curcumin involves multiple residues, it is expected that single mutation would not abolish the effect completely. The close proximity of docked curcumin to the Tyr198 of the inner wall establishes hydrophobic interaction which was reduced in Y198F mutant. This mutant showed lesser sensitivity to curcumin.

N-terminal α helix of VDAC has been implicated in gating [4,8,9]. Although not universally accepted, it is generally believed that transition from closed to open state is accompanied by the conformational movement of N-terminus. The crystal structure of VDAC reveals that the N-terminal helix resides within the pore [7]. Apparently, the α helix occludes the pore in the closed state and it is displaced towards the inner wall of the channel leading to the opening. Therefore, interaction of curcumin to the N-terminus at one end and to the Y198 at the other end restricts the movement of α helix and thereby stabilizes the closed state.

Whether stabilization of VDAC in closed state or in open state is pro-apoptotic is controversial. Pro-apoptotic proteins e.g. Bax and Bak have been reported to induce VDAC-opening. In the similar line, anti-apoptotic Bcl-x_L induced VDAC closure [41,42]. Interestingly, Bcl-x_L has also been shown to induce VDAC opening [43,44]. Optimum opening of VDAC must be important for the exchange of ATP and ADP and thus anti-apoptotic. VDAC prefers anion over cation in the open state. Therefore, Ca^{2+} entry to the mitochondria, a pre-requisite for the induction of mitochondrial permeability transition pore (MPTP) that follows apoptosis, will also be limited in open state. Stabilization of VDAC in the closed state presumably will induce apoptosis due to disruption of normal metabolite flux. This view is supported by the fact that pro-apoptotic protein Bid induces VDAC closure [45]. It has also been shown that in rat liver mitochondria, closure of VDAC increased oxidative stress and accelerated Ca^{2+} mediated MPTP which are considered as pro-apoptotic factors [46]. Therefore, VDAC-closure by curcumin contributes to its well-known pro-apoptotic property. Our study reveals a novel mode of action of curcumin.

Funding sources

This work was supported by LSRB, Defence Research and Development Organisation, Government of India; grant No.DLS/81/48222/LSRB-161/BTB/2008

Conflict of interest

The authors declare no conflict of interest.

Acknowledgments

We sincerely acknowledge Dr. Kornelius Zeath, Max Planck Institute of Biochemistry, Germany for providing VDAC construct. We would like to thank Prashant Kumar, Sucheta, Debayan, Shashipraksh, Amit and Wasima for their valuable suggestions.

Appendix A. Supplementary data

Supplementary data to this article can be found online at http://dx.doi.org/10.1016/j.bbamem.2014.10.014.

References

[1] G. Kroemer, J.C. Reed, Mitochondrial control of cell death, Nat. Med. 6 (2000) 513–519.
[2] A. Messina, S. Reina, F. Guarino, V. De Pinto, VDAC isoforms in mammals, Biochim. Biophys. Acta 1818 (2012) 1466–1476.
[3] V. Shoshan-Barmatz, V. De Pinto, M. Zweckstetter, Z. Raviv, N. Keinan, N. Arbel, VDAC; a multi-functional mitochondrial protein regulating cell life and death, Mol. Aspects Med. 31 (3) (2010) 227–285.
[4] M. Colombini, VDAC structure, selectivity, and dynamics, Biochim. Biophys. Acta 1818 (6) (2012) 1457–1465.
[5] T. Hodge, M. Colombini, Regulation of metabolite flux through voltage-gating of VDAC channels, J. Membr. Biol. 157 (1997) 271–279.
[6] V. Shoshan-Barmatz, D. Ben-Hail, VDAC, a multi-functional mitochondrial protein as a pharmacological target, Mitochondrion 12 (2012) 24–34.
[7] R. Ujwal, D. Cascio, J.P. Colletier, S. Faham, J. Zhang, L. Toro, P. Ping, J. Abramson, The crystal structure of mouse VDAC1 at 2.3 Å. resolution reveals mechanistic insights into metabolite gating, Proc. Natl. Acad. Sci. U. S. A. 105 (2008) 17742–17747.
[8] M. Colombini, Voltage gating in the mitochondrial channel, VDAC, J. Membr. Biol. 111 (1989) 103–111.
[9] B. Mertins, G. Psakis, W. Grosse, K.C. Back, A. Salisowski, P. Reiss, U. Koert, L.O. Essen, Flexibility of the N-terminal mVDAC1 segment controls the channel gating behavior, PLoS One 7 (2012) e47938.
[10] J. Song, C. Midson, E. Blachly-Dyson, M. Forte, M. Colombini, The sensor regions of VDAC are translocated from within the membrane to the surface during the gating processes, Biophys. J. 74 (1998) 2926–2944.
[11] M. Colombini, E. Blachly-Dyson, M. Forte, VDAC, a channel in the outer mitochondrial membrane, Ion Channels 4 (1996) 169–202.
[12] V. De Pinto, S. Reina, F. Guarino, A. Messina, Structure of the voltage-dependent anion channel; state of the art, J. Bioenerg. Biomembr. 40 (2008) 139–147.
[13] S. Hiller, G. Wagner, The role of solution NMR in the structure determinations of VDAC-1 and other membrane proteins, Curr. Opin. Struct. Biol. 19 (2009) 396–401.
[14] O.P. Choudhary, R. Ujwal, W. Kowallis, R. Coalson, J. Abramson, M. Grabe, The electrostatics of VDAC: implications for selectivity and gating, J. Mol. Biol. 396 (2010) 580–592.
[15] O. Teijido, R. Ujwal, C.O. Hillerdal, L. Kullman, T.K. Rostovtseva, J. Abramson, Affixing N-terminal α-helix to the wall of the voltage-dependent anion channel does not prevent its voltage gating, J. Biol. Chem. 287 (2012) 11437–11445.
[16] D.R. Green, J.C. Reed, Mitochondria and apoptosis, Science 281 (1998) 1309–1311.
[17] S. Ma, C. Hockings, K. Anwari, T. Kratina, S. Fennell, M. Lazarou, M.T. Ryan, R.M. Kluck, G. Dewson, Assembly of the Bak apoptotic pore: a critical role for the Bak protein α6 helix in the multimerization of homodimers during apoptosis, J. Biol. Chem. 288 (2013) 26027–26038.
[18] A. Schindler, E. Foley, Hexokinase 1 blocks apoptotic signals at the mitochondria, Cell. Signal. 25 (2013) 2685–2692.
[19] V. Shoshan-Barmatz, N. Keinan, H. Zaid, Uncovering the role of VDAC in the regulation of cell life and death, J. Bioenerg. Biomembr. 40 (2008) 183–191.
[20] A.D. Chacko, F. Liberante, I. Paul, D.B. Longley, D.A. Fennell, Voltage dependent anion channel-1 regulates death receptor mediated apoptosis by enabling cleavage of caspase-8, BMC Cancer 20 (10) (2010) 380.
[21] R. Rizzuto, D. De Stefani, A. Raffaello, C. Mammucari, Mitochondria as sensors and regulators of calcium signalling, Nat. Rev. Mol. Cell Biol. (2012) 566–578.
[22] C. Garrido, L. Galluzzi, M. Brunet, P.E. Puig, C. Didelot, G. Kroemer, Mechanisms of cytochrome c release from mitochondria, Cell Death Differ. 13 (2006) 1423–1433.
[23] J.G. Pastorino, J. Hoek, Regulation of hexokinase binding to VDAC, J. Bioenerg. Biomembr. 40 (2008) 171–182.
[24] N. Arbel, D. Ben-Hail, V. Shoshan-Barmatz, Mediation of the antiapoptotic activity of Bcl-xL protein upon interaction with VDAC1 protein, J. Biol. Chem. 287 (2012) 23152–23161.
[25] Y. Zheng, C. Tian, C. Jiang, H. Jin, J. Chen, A. Almasan, H. Tang, Q. Chen, Essential role of the voltage-dependent anion channel (VDAC) in mitochondrial permeability transition pore opening and cytochrome c release induced by arsenic trioxide, Oncogene 12 (23) (2004) 1239–1247.
[26] N. Tajeddine, L. Galluzzi, O. Kepp, E. Hangen, E. Morselli, L. Senovilla, N. Araujo, G. Pinna, N. Larochette, N. Zamzami, N. Modjtahedi, A. Harel-Bellan, G. Kroemer, Hierarchical involvement of Bak, VDAC1 and Bax in cisplatin-induced cell death, Oncogene 27 (2008) 4221–4232.
[27] B.B. Aggarwal, A. Kumar, A.C. Bharti, Anticancer potential of curcumin: preclinical and clinical studies, Anticancer Res. 23 (2003) 363–398.
[28] S. Reuter, S. Eifes, M. Dicato, B.B. Aggarwal, M. Diederich, Modulation of anti-apoptotic and survival pathways by curcumin as a strategy to induce apoptosis in cancer cells, Biochem. Pharmacol. 76 (2008) 1340–1351.

[29] A. Shehzad, Y.S. Lee, Molecular mechanisms of curcumin action: signal transduction, Biofactors 39 (2013) 27–36.
[30] Z. Xuemei, C. Qijing, W. Yunman, P. Wen, C. Hui, Effects of curcumin on ion channels and transporter, Front. Physiol. 5 (2014) 94.
[31] A. Scharstuhl, H.A. Mutsaers, S.W. Pennings, F.G. Russel, F.A. Wagener, Involvement of VDAC, Bax and ceramides in the efflux of AIF from mitochondria during curcumin-induced apoptosis, PLoS One 4 (2009) e6688.
[32] H. Engelhardt, T. Meins, M. Poynor, V. Adams, S. Nussberger, W. Welte, K. Zeth, High-level expression, refolding and probing the natural fold of the human voltage-dependent anion channel isoforms I and II, J. Membr. Biol. 216 (2007) 93–105.
[33] F. Palmieri, V. De Pinto, Purification and properties of voltage dependent anion channel of the outer mitochondrial membrane, J. Bioenerg. Biomembr. 4 (1989) 417–425.
[34] U.K. Laemmli, Cleavage of structural proteins during the assembly of the head of bacteriophage T4, Nature 227 (1970) 680–685.
[35] A.K. Bera, S. Ghosh, S. Das, Mitochondrial VDAC can be phosphorylated by cyclic AMP-dependent protein kinase, Biochem. Biophys. Res. Commun. 209 (1995) 213–217.
[36] G.M. Morris, R. Huey, W. Lindstrom, M.F. Sanner, R.K. Belew, D.S. Goodsell, A.J. Olson, AutoDock4 and AutoDockTools4: automated docking with selective receptor flexibility, J. Comput. Chem. 30 (2009) 2785–2791.
[37] M. Bayrhuber, T. Meins, M. Habeck, S. Becker, K. Giller, S. Villinger, C. Vonrhein, C. Griesinger, M. Zweckstetter, K. Zeth, Structure of the human voltage-dependent anion channel, Proc. Natl. Acad. Sci. U. S. A. 105 (2008) 15370–15375.
[38] Y. Jen, A.B. Thomas, G. Chi-Chen, L. Choh-Hao, Conformation of β-endorphin and β-lipotropin: formation of helical structure in methanol and sodium dodecyl sulfate solutions, Proc. Natl. Acad. Sci. U. S. A. 74 (1977) 3235–3238.
[39] S. Narasimha, W.W. Robert, Estimation of protein secondary structure from circular dichroism spectra: comparison of CONTIN, SELCON, and CDSSTR methods with an expanded reference set, Anal. Biochem. 287 (2000) 252–260.
[40] S.P. Mitra, Binding and stability of curcumin in presence of bovine serum albumin, J. Surf. Sci. Technol. 23 (2007) 91–110.
[41] S. Shimizu, M. Narita, Y. Tsujimoto, Bcl-2 family proteins regulate the release of apoptogenic cytochrome c by the mitochondrial channel VDAC, Nature 399 (1999) 483–487.
[42] Y. Tsujimoto, S. Shimizu, VDAC regulation by the Bcl-2 family of proteins, Cell Death Differ. 7 (2000) 1174–1181.
[43] M.G. Vander-Heiden, X.X. Li, E. Gottleib, R.B. Hill, C.B. Thompson, M. Colombini, Bcl-x_L promotes the open configuration of the voltage-dependent anion channel and metabolite passage through the outer mitochondrial membrane, J. Biol. Chem. 276 (2001) 19414–19419.
[44] M.G. Vander Heiden, N.S. Chandel, P.T. Schumacker, C.B. Thompson, Bcl-xL Prevents cell death following growth factor withdrawal by facilitating mitochondrial ATP/ADP exchange, Mol. Cell 3 (1999) 159–167.
[45] T.K. Rostovtseva, B. Antonsson, M. Suzuki, R.J. Youle, M. Colombini, S.M. Bezrukov, Bid, but not Bax, regulates VDAC channels, J. Biol. Chem. 279 (2004) 13575–13583.
[46] A. Tikunov, C.B. Johnson, P. Pediaditakis, N. Markevich, J.M. Macdonald, J.J. Lemasters, E. Holmuhamedov, Closure of VDAC causes oxidative stress and accelerates the Ca^{2+} induced mitochondrial permeability transition in rat liver mitochondria, Arch. Biochem. Biophys. 495 (2010) 174–181.